

Dual-wavelength femtosecond Tm: $LuYO_3$ ceramic laser in-band pumped by 1650 nm Er:YAG laser

Jinfang Yang(杨金芳), Purui An(安浦瑞), Chao Bi(毕超), Taotao He(何涛涛), Shichao Yuan(袁诗超), Xinye Tian(田新叶), Man Wan(汪满), Yongle Zhu(朱永乐), Zhong Dong(董忠), and Weijun Ling(令维军)

Citation: Chin. Phys. B, 2026, 35 (**7**): 074202. DOI: 10.1088/1674-1056/ae1fe4
http://cpb.iphy.ac.cn; http://iopscience.iop.org/cpb

What follows is a list of articles you may be interested in

Autocorrelation-based convolutional neural network for reconstruction of noisy attosecond streaking traces

Xiaoxian Zhu(朱孝先), Yitan Gao(高亦谈), Yiming Wang(王一鸣), Kun Zhao(赵昆), and Zhiyi Wei(魏志义)
Chin. Phys. B, 2026, 35 (**5**): 054204. DOI: 10.1088/1674-1056/ae3474

Role of trajectory symmetry in solid high-order harmonic generation

Shuang Wang(王爽), Yu Zhao(赵宇), Hui-Rong Wang(王慧荣), Yun-He Xing(邢云鹤), Xiao-Xin Huo(霍晓鑫), and Jun Zhang(张军)
Chin. Phys. B, 2026, 35 (**4**): 044204. DOI: 10.1088/1674-1056/ae04da

Dissipative soliton operation in a mode-locked laser based on thulium-doped fiber

Wen-Yan Zhang(张文艳), Lei Zheng(郑磊), Tian Zhang(张添), Nan-Nan Liu(刘楠楠), Li-Jie Geng(耿利杰), Kun Yang(杨坤), and Li Zhan(詹黎)
Chin. Phys. B, 2026, 35 (**4**): 044201. DOI: 10.1088/1674-1056/ae063c

Optical temporal interference model for investigation and manipulation of non-integer high-order harmonic generation

Zhao-Yue Meng(孟昭越), Yun Pan(潘云), Jun-Ping Wang(王军平), and Xi Zhao(赵曦)
Chin. Phys. B, 2026, 35 (**2**): 024208. DOI: 10.1088/1674-1056/adfdc5

A 12.1-W SESAM mode-locked Yb:YAG thin disk laser

Yingnan Peng(彭英楠), Zhaohua Wang(王兆华), Dehua Li(李德华), Jiangfeng Zhu(朱江峰), Zhiyi Wei(魏志义)
Chin. Phys. B, 2016, 25 (**5**): 054205. DOI: 10.1088/1674-1056/25/5/054205

Dual-wavelength femtosecond Tm:$LuYO_3$ ceramic laser in-band pumped by 1650 nm Er:YAG laser

Jinfang Yang(杨金芳)[1,2], Purui An(安浦瑞)[1,2], Chao Bi(毕超)[1,2], Taotao He(何涛涛)[1,2], Shichao Yuan(袁诗超)[1,2], Xinye Tian(田新叶)[1,2], Man Wan(汪满)[1,2], Yongle Zhu(朱永乐)[1,2], Zhong Dong(董忠)[1,2], and Weijun Ling(令维军)[1,2,3,†]

[1] *Gansu Provincial All Solid-State Laser Engineering Research Center, Tianshui Normal University, Tianshui* 741001, *China*
[2] *Engineering Research Center of Integrated Circuit Packaging and Testing, Ministry of Education, Tianshui* 741001, *China*
[3] *Gansu Integrated Circuit Packaging and Testing Industry Research Institute, Tianshui* 741001, *China*

(Received 10 September 2025; revised manuscript received 13 November 2025; accepted manuscript online 17 November 2025)

An in-band pumped dual-wavelength femtosecond Tm:$LuYO_3$ ceramic laser is demonstrated for the first time, to the best of our knowledge. In the continuous wave (CW) regime, a maximum output power of 1.03 W with a slope efficiency of 28.7% is obtained; the center wavelength can be independently tuned within the range of 1962 nm to 2070 nm using output couplers (OCs) with different transmittance rates. A single-wavelength laser at 2059 nm is achieved with the shortest pulse duration of 313 fs, a maximum average output power of 374 mW, and operating at a repetition rate of 93.13 MHz. Using a 3% OC, dual-wavelength femtosecond pulses at 1950 nm and 2047 nm were simultaneously generated. Furthermore, the phenomenon of wavelength redshift was observed as the pump power was increased. These experimental results indicate that in-band pump technology combined with Tm:$LuYO_3$ ceramics could be a potential means to reduce the thermal effect and scale the output power and conversion efficiency for 2 μm ultrafast lasers.

Keywords: 2 μm dual-wavelength femtosecond laser, Tm:$LuYO_3$ ceramic, SESAM mode-locked, in-band pumping technology

PACS: 42.65.Re, 42.72.Ai

DOI: 10.1088/1674-1056/ae1fe4 **CSTR:** 32038.14.CPB.ae1fe4

1. Introduction

Dual-wavelength Tm-doped femtosecond lasers have significant application value in fields such as high-resolution laser lidar, precision medical surgery, and material processing.[1–4] The two-wavelength beat frequency technique can generate terahertz waves in specific frequency bands, expanding the spectral coverage ranges and providing a new technical means for material spectral analysis.[5–8]

The Tm^{3+}:Re_2O_3 sesquioxide, with its comprehensive advantages of wide transmittance (0.2–8 μm), low phonon energy (suppressing non-radiative transitions and extending fluorescence lifetime), wide emission bandwidth (1.8–2.1 μm), and excellent thermal stability (slightly lower than YAG), has become the core candidate material for mid-infrared high-power, short-pulse-duration lasers.[9] Among the various Tm^{3+}:Re_2O_3 sesquioxides (e.g., Tm:Y_2O_3, Tm:$LuScO_3$), Tm:$LuYO_3$ ceramic has the potential to excel because it combines two very significant properties: the inherent multi-site cation substitution effect within this host, coupled with strong interactions with the crystalline lattice field, induces significant spectral inhomogeneity broadening. A large emission cross section (0.8×10^{-20} cm^2) and a wide emission bandwidth ($>$ 80 nm) support the generation of sub-100 fs pulses, and the high thermal conductivity (12 W/m·K^{-1}) allows for high-power pumping.[10–14] By fine-tuning the ratio of Lu^{3+} and Y^{3+}, the energy level splitting and Stark broadening of Tm^{3+} can be flexibly controlled, thereby forming two independent gain peaks that support dual-wavelength femtosecond pulse oscillation.

Currently, the pump sources for generating 2 μm lasers include 793 nm Ti:sapphire lasers and laser diodes (LDs), and 1650 nm Er:YAG lasers.[15–19] Although LDs are inexpensive and compact, they have low brightness, poor beam quality, and low quantum conversion efficiency, making it difficult to achieve mode locking. Most Tm-doped ultrafast laser systems, especially Tm:$LuYO_3$ lasers, are pumped by Ti:sapphire lasers, mainly due to their high brightness and easy mode-locking characteristics, which can generate ultrashort pulses as short as sub-60 fs.[20–22] In 2019, Li *et al.* reported a 796 nm LD-pumped semiconductor saturable absorber mirror (SESAM) mode-locked Tm:$LuYO_3$ laser, delivering 1.2 W, 41 ps pulses.[14] In 2020, Zhao *et al.* demonstrated a Ti:sapphire laser centered at 795.3 nm pumped Tm:$LuYO_3$ laser, generating ultrashort pulses as short as 54 fs, which was the shortest pulse duration based on Tm:$LuYO_3$ ceramic. The corresponding average power was only 51 mW.[19] In 2023, our research group reported a direct Kerr lens mode-locked Tm:$LuYO_3$ ceramic laser without any mode-locking

†Corresponding author. E-mail: wjlingts@sina.com

© 2026 Chinese Physical Society and IOP Publishing Ltd. All rights, including for text and data mining, AI training, and similar technologies, are reserved.

initiation elements, achieving pulse durations as short as 259 fs and a maximum average output power of 326 mW.[13] In summary, due to the low output power, large size, high cost, and especially the low quantum conversion efficiency (below 40%) and severe thermal lensing effect of Ti:sapphire lasers, there is an urgent need to find another, higher-quality pump source.[23]

The 1650 nm laser in-band pumping technology has demonstrated great potential in the generation of high-power 2 μm lasers. The 1650 nm pumping wavelength corresponds to the $^3H_6 \rightarrow ^3F_4$ absorption transition of Tm^{3+}, directly pumping the ions to the laser upper energy level $^3F_4$. This method utilizes Stark splitting to create sub-level branches, enabling laser emission between these branches. Due to the small energy difference between the pump photons (approximately 1.52×10^{-19} J) and the laser photons (approximately 1.0×10^{-19} J), the quantum conversion efficiency theoretically approaches 100%.[24–27] In addition, Tm-doped crystals have a large absorption cross section (1–5 $\times10^{-20}$ cm^2) for 1650 nm pump lasers and a wide absorption bandwidth (50–100 nm), and do not require stringent pump-wavelength stability. Currently, there have been some reports on in-band pumping of Tm-doped lasers, but, so far, there have been no reports on a 1650 nm in-band pumping $Tm:LuYO_3$ femtosecond laser.

In this work, we report for the first time a dual-wavelength SESAM mode-locked $Tm:LuYO_3$ ceramic laser, in-band pumped by a 1650 nm Er:YAG laser. In the continuous wave (CW) regime, a maximum output power of 1.03 W is obtained with a 9% output coupler (OC) at a pump power of 9.26 W, corresponding to a slope efficiency of 28.7%. The center wavelength could be discretely selected across a range from 1962 nm to 2070 nm by swapping OCs with different transmittances. In the mode-locked single-wavelength regime, the maximum average output power reaches 374 mW at a repetition rate of 93.13 MHz, and the measured pulse duration is 353 fs. The shortest pulse duration is 313 fs, but the output power is only 51 mW at a center wavelength of 2059 nm. Using the 3% OC, dual wavelengths were centered around 1950 nm and 2047 nm, and red-shifts of the lasing wavelengths were observed with the increase of the pump power.

2. Experimental setup

The experimental configuration of the dual-wavelength mode-locked $Tm:LuYO_3$ ceramic laser is illustrated schematically in Fig. 1. The pump source is a solid-state Er:YAG laser emitting at 1650 nm, with a maximum average power of 11 W. A 4 at.% Tm^{3+}-doped $LuYO_3$ ceramic ($3\times3\times4.4$ mm^3), cut at the Brewster angle with polished end-faces, serves as the gain medium. This Brewster-angle orientation enhances optical damage resistance while minimizing reflection losses. To mitigate thermal lensing and prevent fracture, the crystal was encapsulated in indium foil and mounted in a water-cooled copper block maintained at 13 °C via a recirculating chiller. The 1650 nm pump laser was focused into the crystal using a 100 mm focal length lens (L) with > 95% transmittance at the pump wavelength. Two flat mirrors are used for collimation and propagation of the pump beam.

The linear resonator (Fig. 1) comprises two dichroic concave mirrors (M1, M2; ROC = 100 mm), plane mirrors (M3, M5), a plano-concave mirror (M4, ROC = 100 mm), and a planar output coupler (OC). Dispersion compensation was implemented via two intracavity chirped mirrors (CMs; CM1, CM2), each providing -200 fs^2 of group delay dispersion (GDD) per bounce. Round-trip GDD values of -400 fs^2 (single reflection) and -800 fs^2 (double reflection) were achieved by controlled bounce configurations. The resonator's length was maintained at $\sim$ 1.5 m to establish a 93.13 MHz repetition rate.

The laser resonator is designed as an x-type cavity, which helps to reduce the oscillating pulse spot size at the gain medium and lower the mode-locking threshold. The SESAM was inserted into the cavity to initiate mode-locking. In our configuration, the SESAM serves as the indispensable component for starting and stabilizing the pulsed operation, providing the necessary nonlinear loss modulation. Only when the distance between the SESAM and the M4 concave mirror is between 53 mm and 55 mm can the $Tm:LuYO_3$ laser realize mode-locking. If the distance exceeds this range, mode-locking cannot be achieved. Considering the influence of the laser polarization state on the crystal absorption rate, a half-wave plate (HWP) is used to convert the light beam entering the resonator to a P-polarized laser. Based on an *ABCD* matrix, the spot radius of the oscillating pulse is 35 μm, and the spot size of the pump beam focused in the crystal is 38.5 μm, which provides good mode-matching at the crystal.

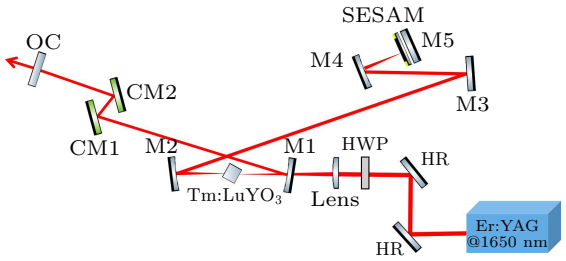


Fig. 1. The experimental setup of $Tm:LuYO_3$ ceramic mode-locked laser with in-band pumping scheme.

3. Experimental results and discussion

Initially, we investigated the output performance of a $Tm:LuYO_3$ laser in the CW regime using six different OCs with transmissions of 0.5%, 1.0%, 1.5%, 3.0%, 5%, and 9%. Figure 2 shows the CW laser output power versus pump power for different OCs. With the 0.5%, 1.0%, and 1.5% OCs, the lowest pump threshold was as low as 700 mW for CW lasing.

As the transmittance rates of the OCs increased, the slope efficiency also increased from 6.4% to 29.3%. The maximum slope efficiency was 29.3% with a 5.0% OC, and the average output power was 920 mW at 4 W absorbed pump power. This was mainly due to the fact that the output power actually decreases at higher pump powers. To avoid damaging the crystal, the pump power was not increased further. The maximum CW output power was 1.03 W at an average power of 9.26 W using a 9% OC. The measured maximum slope efficiency was lower than the theoretical values. The primary limiting factors were as follows. (1) After the pump laser was absorbed, some particles may release energy as phonons during the transition to the laser's upper energy level by non-radiative transitions, which prevented the energy from being effectively utilized for laser oscillation. (2) Absorption, scattering, and incomplete reflection at the output mirror within the laser cavity consumed laser energy, requiring increased pump power to sustain oscillation. (3) High pump power generated thermal effects that altered the refractive index of the laser medium, degrading the beam quality. This may also modify the energy level structure of Tm^{3+} ions, reducing laser gain and consequently lowering the quantum conversion efficiency.

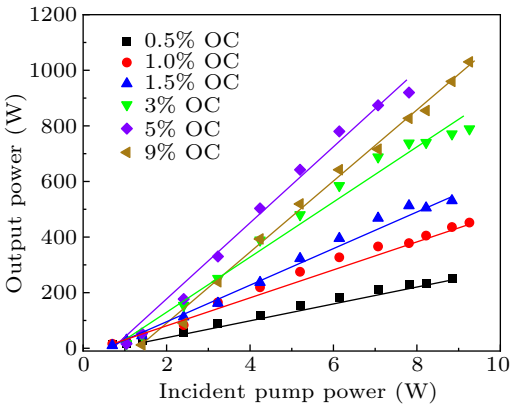


Fig. 2. The output power versus pump power for a CW Tm:$LuYO_3$ mode-locked laser.

Table 1. Summary of a CW laser operations with different transmittance rate OCs.

Transmittance rates of OCs	Pump threshold (W)	Output power (W)	Slope efficiency
0.5%	0.7	0.250	6.4%
1.0%	0.7	0.452	12.3%
1.5%	0.7	0.531	14.5%
3.0%	0.82	0.789	22.3%
5.0%	1.04	0.920	29.3%
9%	1.04	1.030	28.7%

In the CW regime, spectral measurements were performed using a spectrometer (AvaSpec-NIR256-2.5TEC, Avantes) with a specified resolution range of 6–90 nm. The spectral characterization revealed a systematic output redshift with decreasing OC transmittance (Fig. 3). The emission peak wavelength shifted from 1962 nm at TOC = 5% to 2070 nm at TOC = 0.5%, representing a 108 nm wavelength shift. When the OC transmittance decreased, cavity losses diminished while gain increased. This caused the laser oscillation mode to shift toward longer wavelengths with higher gain, resulting in a wavelength redshift. When OC transmittance dropped from 5% to 3%, cavity losses were significantly reduced, leading to a marked increase in the laser medium gain. At this point, certain longer-wavelength, higher-gain modes that were previously suppressed due to high loss became excited. These new modes exhibited significant wavelength differences from the original modes, resulting in a large redshift span. As transmittance decreased from 3% to 0.5%, cavity loss became very low, laser oscillation stabilized, and the primary oscillation mode was established. Further reduction in transmittance still increased gain, but its effect on the mode diminished. New modes became difficult to excite significantly, causing the wavelength redshift span to slow.

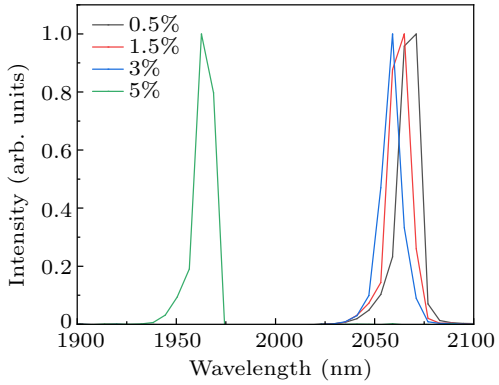


Fig. 3. The CW laser spectra with different transmittance rate OCs.

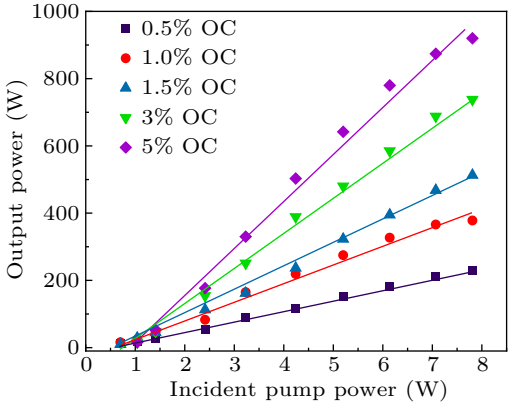


Fig. 4. The average output power of mode-locked Tm:$LuYO_3$ ceramic laser with different transmittance rate OCs.

For mode-locking operation, a SESAM was placed at the focus of an M4 concave mirror to create a second intracavity beam waist to activate mode-locking. Systematic evaluation of mode-locking performance across different OCs with different transmittance rates was conducted by integrating the SESAM and CMs into the resonator. Stable CW mode-locking was achieved with 0.5%, 1%, 1.5%, and 3% OCs. Figure 4 presents the corresponding average output power characteristics under various operational conditions, demonstrating distinct power-scaling behavior for each OC configuration. Fol-

lowing systematic dispersion compensation optimization, Table 2 quantifies the mode-locking performance across different OCs. Comparative analysis reveals a consistent trend: decreasing OC transmittance simultaneously reduces the mode-locking threshold, increases average output power, and extends pulse duration. This tripartite correlation stems fundamentally from enhanced intracavity intensity at lower TOC, which promotes saturable absorber action while prolonging photon lifetime and spectral filtering effects.

Table 2. The performance of Tm:$LuYO_3$ ceramic mode-locked laser with different transmittance rate OCs.

Transmittance rates of the OCs	Mode-locking threshold (W)	Average power (mW)	Pulse duration (fs)
0.5%	3.41	52	313
1.0%	3.10	108	334
1.5%	3.10	225	348
3%	2.71	374	353

With 3% OC, the average power reached up to 374 mW, and the corresponding pulse duration was 353 fs. However, the SESAM surface is easily damaged, leading to unstable mode-locking and incomplete data measurement. For an absorbed pump power of 3.41 W, pulses as short as 313 fs with an average output power of 51 mW were obtained directly from the mode-locked Tm:$LuYO_3$ laser with 0.5% OC at a repetition rate of 93.13 MHz. This was the shortest pulse duration based on a Tm:$LuYO_3$ laser in this work. Therefore, we investigated the laser performance based on the above conditions.

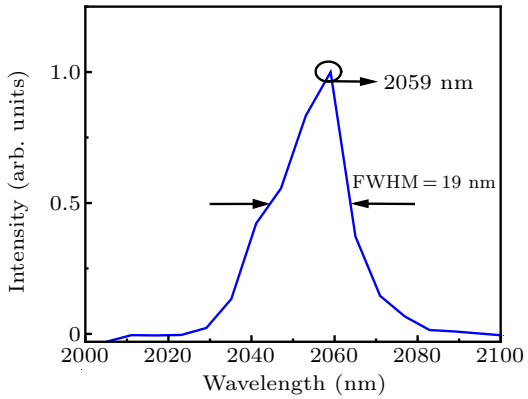


Fig. 5. The output spectrum obtained in mode-locked regimes.

Fig. 5 displays the corresponding optical spectrum centered at $\lambda = 2059$ nm; the FWHM was 19 nm, and the theoretical limited pulse duration was 296 fs. Temporal characterization via intensity autocorrelation (pulseCheck APE, APE GmbH) yielded the trace in Fig. 6. Assuming a sech^2 pulse profile, the measured pulse duration was 313 fs, which was close to the limiting pulse duration. Specifically, due to the extremely low transmittance of 0.5% OC, the photon lifetime within the cavity is significantly prolonged, and the cavity energy accumulation efficiency is enhanced, thereby strengthening the nonlinear effect. However, the low transmittance simultaneously limits the effective output of laser energy, ultimately resulting in the average output power being significantly lower than the experimental results under the conditions of high transmittance OC (such as 3% or 5%).

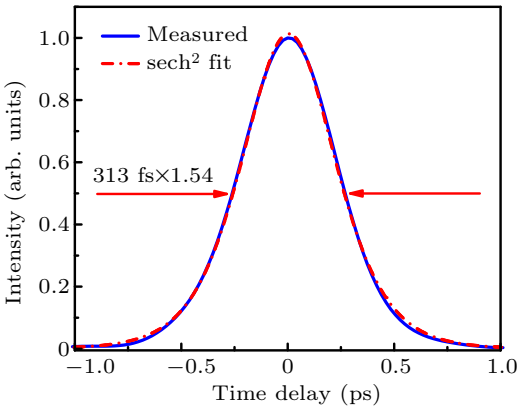


Fig. 6. The measured autocorrelation trace of the mode-locking Tm:$LuYO_3$ ceramic laser.

These experimental results clearly demonstrate that the choice of output mirror transmittance significantly affects the central wavelength, output power, and mode-locking threshold of the laser. According to the formula $\tau_p \propto \sqrt{T+L}$, here, τ_p represents the pulse duration, T is the transmittance of the output mirror, and L is the linear loss within the cavity. Although OCs with lower transmittance require higher pump power to achieve mode-locking, they can provide a higher intracavity photon density, effectively enhancing the photon lifetime within the cavity. This promotes the accumulation of nonlinear effects and optimizes mode-locking stability, which is beneficial for the initiation and maintenance of mode-locking. However, excessively low output transmittance can also lead to increased intracavity losses, thereby limiting the improvement of output power. Additionally, the slight shift in the central wavelength may be related to intracavity dispersion compensation and the thermal effects of the gain medium, the specific mechanisms of which require further investigation.

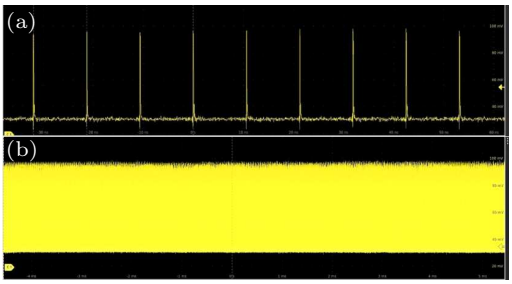


Fig. 7. The typical mode-locked pulse trains in 10 ns scanning time (a) and 1 ms scanning time (b).

Temporal characterization of the mode-locked pulse train was performed using a high-bandwidth photodetector (ET-5000, Electro-Optics Technology, 12.5 GHz bandwidth) coupled to an 8-GHz digital oscilloscope (MSO6, Tektronix, Inc.). Optimal signal integrity was achieved through photodiode bias

optimization and oscilloscope triggering synchronization. Figures 7(a) and 7(b) demonstrate stable CW mode-locking operation, with Fig. 7(a) resolving individual pulse separation over a 10-ns window and Fig. 7(b) confirming long-term stability (>1 ms duration) without Q-switching instabilities or amplitude modulation.

The recorded RF spectrum, acquired with resolution bandwidth (RBW) settings of 100 kHz and 300 Hz, demonstrated that the fundamental tone at 93.13 MHz exceeds the background noise floor by more than 62 dB. This spectral dominance is illustrated in Fig. 8.

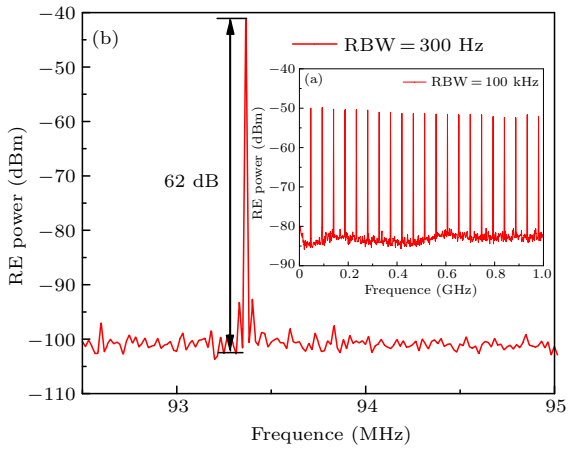


Fig. 8. Typical RF spectrum of the Tm:$LuYO_3$ femtosecond laser with the RBW of 100 kHz. Inset: RF spectrum at 1 GHz wide-span with the RBW of 300 Hz.

Furthermore, experimental observations revealed a dual-wavelength emission regime in the mode-locked laser system. Figure 9 depicts the dual-wavelength spectral evolution with the increase of the pump powers using 3% OC. It is worth noting that as the pump power increased, a redshift phenomenon appeared for the dual-wavelength pulses. When the pump power was 7.07 W, the maximum output power at the dual wavelengths of 1962 nm and 2059 nm was 200 mW. A pulse duration of 353 fs was measured for the dual-wavelength operation, representing the collective pulse duration of the composite output that includes both wavelength components. In addition, the dual wavelength could only be generated when the pump power was between 4.42 W and 7.07 W. The Tm:$LuYO_3$ ceramic dual-wavelength femtosecond lasers are generated by the simultaneous oscillation and amplification of two different wavelength laser modes under specific conditions. The core mechanism involves rare earth ion energy level transitions, gain characteristic control, mode competition balance, and dispersion management. Dual-wavelength lasers share the same gain resources in the Tm:$LuYO_3$ ceramic, and their gain competition relationship dynamically adjusts with changes in parameters such as pump power and cavity loss. In addition, the Tm:$LuYO_3$ ceramic lattice field causes significant Stark splitting of the $^3F_4$ and $^3H_6$ energy levels, forming multiple sub-energy levels. Stimulated radiation transitions between these different sub-energy levels generate dual-wavelength lasers.

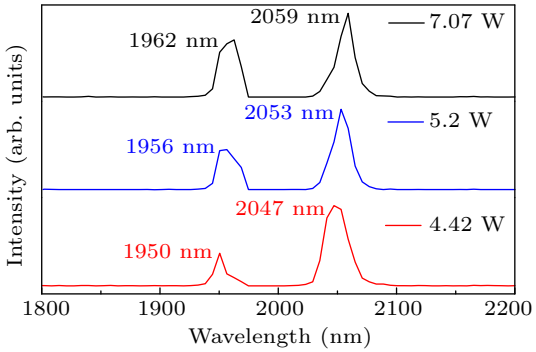


Fig. 9. The measured dual-wavelength spectrum of the mode-locking Tm:$LuYO_3$ ceramic laser with different pump powers.

4. Conclusion

In conclusion, an in-band pumped dual-wavelength Tm:$LuYO_3$ ceramic mode-locked laser was experimentally demonstrated for the first time. In CW operation, the maximum output power was as high as 1.03 W with a slope efficiency of 28.7% at a pump power of 9.26 W using a 9% OC. The CW center wavelength can be tuned from 1962 nm to 2070 nm using OCs with different transmittance rates. Based on SESAM mode-locking, results with 374 mW, 353 fs and 51 mW, 313 fs pulses were obtained from the Tm:$LuYO_3$ laser. A dual-wavelength femtosecond laser was achieved and was tunable from 1950 nm, 2047 nm to 1962 nm, 2059 nm using different OCs. We believe that this work opens a new way to realize a higher-power, higher-conversion-efficiency mid-infrared dual-wavelength ultrafast laser.

Acknowledgements

This work was supported by TheNational Natural Science Foundation of China (Grant Nos. 62405221 and 62165012), Gansu Province University Industry Support Plan Project (Grant No. 2024CYZC-44), Key Talent Project of Gansu Province (Grant No. 2025RCXM023), Major Cultivation Project of University Research and Innovation Platform of Gansu Provincial Department of Education (Grant No. 2024CXPT-12), Tianshui Strong Science and Technology Award Special Project (Grant No. TS-STK-2024A-277), Qinzhou District Science and Technology Plan Project (Grant No. 2024-SHFZG-8159), and Basic Research Program of Gansu Provincial Science and Technology Plan (Grant Nos. 25JRRE009, 25JRZE003, and 25JRRE003).

References

[1] He X, Hao Q Q, Wang H L, Yu S, Zhou Y, Guo B and Li L J 2024 *Laser Photon. Rev.* **18** 2300588
[2] Targ R, Steakley B C, Hawley J G, Ames L L and Robinson P A 1996 *Applied Optics* **35** 007117

[3] Liu B, Li X, Dong J, Zhang L and Li L 2025 *Chin. Phys. B* **34** 094208

[4] Dong J H, Zhang C, Zhao Y H, Long C Y, Wang N, Liu J and Liu J J 2022 *Infrared Physics & Technology* **123** 104189

[5] Liu P, Lin J, Liu X, Huang H T, Zhang J, Tang D Y and Shen D Y 2016 *IEEE Photonics Journal* **8** 1504007

[6] Liu X Y, Li X W, Zhao S Z, Yang K J, Guo L, Li T, Qiao W C, Li M, ZhangB T, He J L, Zheng L H, Su L B and Xu J 2019 *Chin. Opt. Lett* **17** 091401

[7] Kong L C, Qin Z P, Xie G Q, Xu X D and Yuan L J 2015 *Opt. Lett.* **40** 356

[8] Huang H T, Wang S Q, Chen H W, Antipov O L, Balabanov S S and Shen D Y 2019 *Opt. Express* **27** 38593

[9] Senatsky Y V, Shirakawa A, Sato Y, Hagiwara J and Yanagitani T Y 2004 *Laser Optics* **88–97** 5478

[10] Yin H W, Li Y F, Yang Y F, Zhu C Y, Li D, Wang G, Hou S P, Yu Y, Wang Y and Lu Z 2025 *Optical Materials* **162** 116888

[11] Chen G Z, Li S M, Zhang L H, Tan X J, Deng W, He M Z, Xu M, Yang Y L, Zhang S L and Hang Y 2020 *Infrared Physics & Technology* **109** 103431

[12] Suzuki A, Kalusniak S, Ganschow S, Kränkel C and Tokurakawa M 2023 *Opt. Lett.* **48** 4221

[13] Ling W J, Xue J W, Yang J F, Wang C, Du X J, Wang W T and Dong Z 2023 *Chin. Phys. B* **32** 114211

[14] Li D Z, Kong L C, Xu X D, Liu P, Xie G Q, Zhang J and Xu J 2019 *Opt. Express* **27** 24416

[15] Zeng H J, Xue W Z, Murray Robert T, Chen C, Wang L, Pan Z B, Pavel L, Xavier M, Yuan F F, Zhang G, Uwe G, Valentin P and Chen W D 2024 *Opt. Express* **32** 16083

[16] Zhang W S, Li L J and Liang H 2025 *Optics & Laser Technology* **181** 111947

[17] Wang L, Chen W D, Zhao Y G, *et al.* 2021 *High Power Laser Science and Engineering* **9** 04000e50

[18] Chen C, Wang C, Li Y, Shangguan J and Feng H L 2024 *Laser Physics* **34** 075003

[19] Chen W, Mero M, Wang Y and Zhao Y 2020 *Applied Optics* **59** 10493

[20] Zhou Z Y, Guan X F, Huang X X, Xu B, Xu H Y, Cai Z P, Xu X D, Liu P, Li D Z, Zhang J and Xu J 2017 *Opt. Lett* **42** 3781

[21] Zhao Y G, Wang L, Wang Y C, *et al.* 2020 *Opt. Lett* **45** 459

[22] Chen G Z, Li S M, Zhang Y H, Zhang S L, Fang Q N, He M Z, Xu M, Zhang M, Pan S L, Hang Y 2021 *Journal of Luminescence* **234** 117951

[23] Zhao G D, Ma J Y, Han H N, Wang Z H, Wei Z Y 2025 *Chin. Phys. B* **34** 084204

[24] Zhang N, Wang Z X, Liu S D, Wei Jing W, Huang H, Huang Z X, Tian K Z, Yang Z Y, Zhao Y G, Griebner U, Petrov V and Chen W D 2022 *Opt. Express* **30** 23978

[25] Zhang N, Wang P F, Chen B, Wang Z X, Liu S D, Zhao Y G, Jia Z T, Zhang B T and Sun Z P 2022 *Appl. Phys. B* **128** 128

[26] Thouroude R, Tyazhev A, Hideur A, Loiko P, Camy P, Doualan J, Gilles H and Laroche M 2020 *Opt. Lett* **45** 4511

[27] Meng Z Q, Liu J L, Zhang J, Chen X Y, Yu Y J and Jin G Y 2025 *Infrared Physics & Technology* **150** 106033